



ACADEMIC  
PRESS

Available online at [www.sciencedirect.com](http://www.sciencedirect.com)

SCIENCE @ DIRECT®

Journal of Sound and Vibration 266 (2003) 711–721

---

---

JOURNAL OF  
SOUND AND  
VIBRATION

---

---

[www.elsevier.com/locate/jsvi](http://www.elsevier.com/locate/jsvi)

# Experimental analysis of the dynamic, mechanical behaviour of a chicken egg

P. Coucke, B. De Ketelaere\*, J. De Baerdemaeker

*Laboratory for Agricultural Machinery and Processing, Department of Agro-Engineering and -Economics,  
Catholic University Leuven, Kasteelpark Arenberg 30, B-3001 Leuven, Belgium*

Received 13 January 2003

---

## Abstract

The dynamic, mechanical behaviour of a chicken egg is assessed. Experimental modal analysis tests revealed several spherical modes in the 2–7 kHz frequency band. An identification of the mode shapes, the resonant frequencies and corresponding damping ratios of these modes is obtained. The study allows the interpretation of the vibration response of an egg excited at its equator with a light mechanical impact which could open the door towards an automated egg inspection system.

© 2003 Elsevier Ltd. All rights reserved.

---

## 1. Introduction

Old poultry farmers checked the mechanical integrity of hatching eggs by placing two eggs in one hand and spinning the eggs around each other while gently impacting both eggs several times. The characteristic sound produced by this impact contains information about the presence of hairline cracks in the shell. Eggs with cracked shell sound dull and highly damped and are consequently rejected from incubation. Intact eggs produce a typical sound, which is consistent when impacting on several places around the equator. In fact, by impacting the eggs in this way, they start to vibrate at one of their resonant frequencies, producing the typical sound. This test gave rise to the idea that the vibration response of eggs after impact excitation could be used to gain knowledge about the structural integrity of the eggshell.

The study of the acoustic vibrations as an indicator of egg and eggshell quality is limited and relatively recent. Sinha et al. [1] reported the use of acoustic resonant frequency analysis in chicken eggs for the detection of *Salmonella enteritidis* bacteria in the egg content. The excitation

---

\*Corresponding author. Tel.: +32-16-32-8593; fax: +32-16-32-8590.

E-mail address: [bart.deketelaere@agr.kuleuven.ac.be](mailto:bart.deketelaere@agr.kuleuven.ac.be) (B. De Ketelaere).

was done at the blunt side of the egg with a piezoelectric crystal and the response is measured with an accelerometer at the opposite side. Yang et al. [2] used the vibrational behaviour of a chemically treated egg as a quality detection method. Bliss [3] and Moayeri [4] detect the local stiffness of the eggshell by analysing the time signal of the impactor after impacting. Multiple measurements distributed over the whole eggshell surface are required to have a global overview of the eggshell strength.

The present study was intended to better understand the vibration characteristics of an egg. For this purpose, an experimental modal analysis was performed on an intact egg. This analysis gives the possibility to visualize the spatial motion of the egg after being impacted. In this way, an optimal test set-up can be created, regarding optimal supporting points of the egg, and the exact positioning of the impactor and the response-measuring device. The study of the vibration behaviour could lead to automated crack detection in eggs, which is at present still a bottleneck in egg quality sorting.

## 2. Materials and methods

### 2.1. Basics of the experimental modal analysis

Modal analysis refers to an experimental or analytical procedure applied in vibration analysis for describing the dynamic behaviour of mechanical structures. The analysis aims to define the basic deformation shapes (mode shapes) of a mechanical structure when excited at one of its natural frequencies. The simplicity and transparency of the method are mainly determined by postulating four conditions for the structure (see for instance, Ref. [5]):

- (1) It is assumed that the behaviour of the mechanical system is linear. The response of the structure to a set of excitation forces acting simultaneously must be equal to the sum of the responses of all the separate forces of the set.
- (2) The structure is time invariant or its intrinsic characteristics remain constant in time.
- (3) The mechanical system should be observable. The measured outputs must yield sufficient information to construct a reliable mathematical model.
- (4) Finally, the structure has to comply with Maxwell's reciprocity principle. Under these conditions, the measurement and excitation point are interchangeable.

Modal analysis has been extensively used in the past for the study of the dynamic mechanical behaviour of spherically shaped fruits [6,7]. The mathematical concept of experimental modal analysis is fully described by Langenakens et al. [8].

The overall dynamic behaviour is described by a set of linear mass–damper spring systems, which can be described by linear second order differential equations of motion [9]:

$$\mathbf{M}\ddot{\mathbf{X}}(t) + \mathbf{C}\dot{\mathbf{X}}(t) + \mathbf{K}\mathbf{X}(t) = \mathbf{F}(t), \quad (1)$$

where  $\mathbf{X}(t)$  is the displacement vector as a function of time,  $\mathbf{M}$  is the mass or inertia matrix,  $\mathbf{C}$  is the viscous damping matrix,  $\mathbf{K}$  is the stiffness matrix and  $\mathbf{F}(t)$  is the external applied force vector as a function of time.

The modal parameters are defined as damped and undamped natural frequencies, damping factors and ratios and the mode shapes extracted from the residue values. In the further experiments the damped natural frequency, the damping ratio and the mode shape of several modes will be analyzed.

The modal model is fully described by a matrix of frequency response functions  $\mathbf{H}(\omega)$  that are obtained by calculating the ratio of the response signal  $\dot{\mathbf{X}}(\omega)$  to the input signal  $\mathbf{F}(\omega)$  in the frequency domain. If the response is measured as a velocity, this transfer function is called a *mobility transfer function*

$$\mathbf{H}(\omega) = \frac{\dot{\mathbf{X}}(\omega)}{\mathbf{F}(\omega)} \tag{2}$$

In a second step, the modal parameters are extracted using non-linear parameter estimation techniques. The estimation of the poles (frequencies and damping) is based on a global estimation technique in the frequency domain called the least-squares complex exponential method.

If  $\mathbf{H}(\omega)$  is the matrix for  $n_i$  input degrees of freedom (DOF) and  $n_o$  output DOF, the expression for each element  $h_{ij}$  can be written as

$$h_{ij}(\omega) = \sum_{k=1}^N \left[ \frac{r_{ijk}}{(j\omega - \lambda_k)} + \frac{r_{ijk}^*}{(j\omega - \lambda_k^*)} \right] \tag{3}$$

The corresponding relation for the time domain is

$$h_{ij}(t) = \sum_{k=1}^N (r_{ijk} \cdot e^{\lambda_k \cdot t} + r_{ijk}^* \cdot e^{\lambda_k^* \cdot t}), \tag{4}$$

where  $h_{ij}(\omega)$  is the frequency response function (FRF) between the response (or output) DOF  $j$  and the reference (or input or excited) DOF  $i$ ,  $h_{ij}(t)$  is the impulse response (IR) between the response DOF  $i$  and the reference (or input or excited) DOF  $j$ ,  $N$  is the number of modes of vibration that contribute to the structure dynamic response within the frequency range of consideration,  $r_{ijk}$  is the residue value for mode  $k$ ,  $r_{ijk}^*$  is the complex conjugate of the residue value of mode  $k$ ,  $\lambda_k$  is the pole value for mode  $k$ , and  $\lambda_k^*$  is the complex conjugate of the pole value for mode  $k$ .

The pole of mode  $k$  can be expressed as

$$\lambda_k = c_k + j \cdot \omega_{dk} \tag{5}$$

were the real part of the complex pole,  $c_k$ , is the damping value of the mode  $k$ . Physical systems always have a strictly negative damping value (amplitude decreasing in time). The imaginary part of the pole,  $\omega_{dk}$ , represents the damped natural frequency of mode  $k$ .

The damping ratio,  $Z$ , is the ratio of the damping value to the critical damping value. The critical damping value is that value beyond which a mode ceases to oscillate and decays exponentially. The damping ratio is usually expressed in %.

$$Z = \frac{c}{c_{crit}} \times 100. \tag{6}$$

The damped natural frequency can also be written as

$$\omega_d = \omega_n \sqrt{1 - Z^2}, \tag{7}$$

where  $\omega_n$  is the undamped natural frequency (rad/s) and  $\omega_d$  is the damped natural frequency (rad/s).

For lightly damped systems such as eggs ( $Z < 3\%$ ), the difference between the damped and undamped natural frequency is negligible and hence in this study the notation  $\omega$  will be used. When the natural frequencies and damping values are known, the residues or mode shape coefficients can be identified using a least-squares frequency domain method.

The residue value  $r_{ijk}$  between a response DOF  $i$  and a reference DOF  $j$  for a mode  $k$  is the product of the mode shape coefficient  $v_{ik}$ , and the modal participation factor  $l_{jk}$  for the corresponding DOFs and mode:

$$r_{ijk} = v_{ik} \cdot l_{jk}. \quad (8)$$

The poles, natural frequencies, damping factors, mode shapes and residues are commonly referred to as modal parameters and can be derived from dynamic experiments on the structure.

## 2.2. Measurement set-up

The measurement set-up is shown in Fig. 1 and has three major parts, namely the product support, the excitation device and the response-measuring device.

### 2.2.1. Product support

A fresh 65 g white chicken egg is used for the modal analysis. During the measurements the support of the egg must be such that the distortion of its natural motion caused by this support is minimal. The choice was made to support the egg with an elastic string. This string is glued to the sharp end of the egg.

### 2.2.2. Excitation

The impact excitation method is chosen for this test because of its fast and simple nature. The egg is manually excited at 42 input points (references) equally distributed over the eggshell surface (Fig. 2). An average of five measurements for each input point is used.

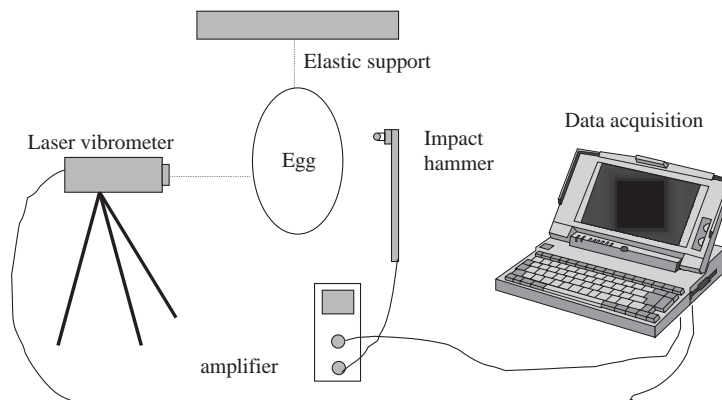


Fig. 1. Schematic design of the experimental set-up.

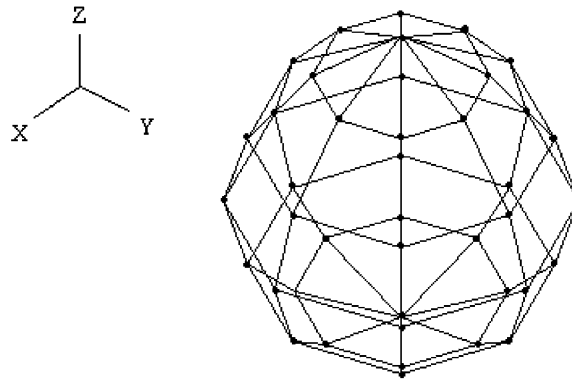


Fig. 2. Isometric view of the 42 excitation nodes on the eggshell.

To obtain an impact signal with a frequency range high enough to excite the frequencies of interest, a small hammer with a stiff steel tip is used. The miniature impact hammer (type GK291C80, PCB Piezotronics Inc., USA) is instrumented with a force transducer with a sensitivity of 27.2 mV/N. The total mass of the hammer is 3 g and its shaft is made of a hollow vinyl tube. The length of the shaft is 6 cm. The tip hardness and weight of the impactor are two characteristics that influence the magnitude and duration of the force pulse width, which in turn determines the magnitude and frequency content of the pulse [10]. Besides these hammer characteristics, the dynamic characteristics of the structure at the impact location and also the manner in which the impact is applied to the structure affects the magnitude and width of the pulse. In this work a repetitive manual excitation was applied after some preliminary tests to assure that a proper frequency content of the force pulse was maintained and that a maximum signal was achieved without instrumentation overload. A typical time signal and the corresponding frequency signal of an impact force excited on an intact chicken egg is shown in Fig. 3.

### 2.2.3. Response measurement

A laser vibrometer (type OFV 3001, Polytec GmBh., Germany) was used to measure the egg response to the impact. This contactless sensor adds no extra mass to the structure and does not disturb the free vibration of the egg. The laser-vibrometer measures the velocity of the vibration at a certain point in the direction of the laser beam. In the test, the laser beam is focused normally to the eggshell surface at a selected node on the equator of the egg. The laser vibrometer is placed on solid concrete and isolated from the egg supporting structure so no disturbing vibrations are introduced when performing the measurements.

### 2.3. Data acquisition and analysis

The data acquisition is controlled using a dual channel Dynamic Signal Analyser (type HP35665A, Hewlett Packard Inc., USA). The signal of the force sensor is windowed by a rectangular window and used for triggering. An exponential decay window filters the response signal. Both signals are transformed to the frequency domain using an FFT. This Fourier

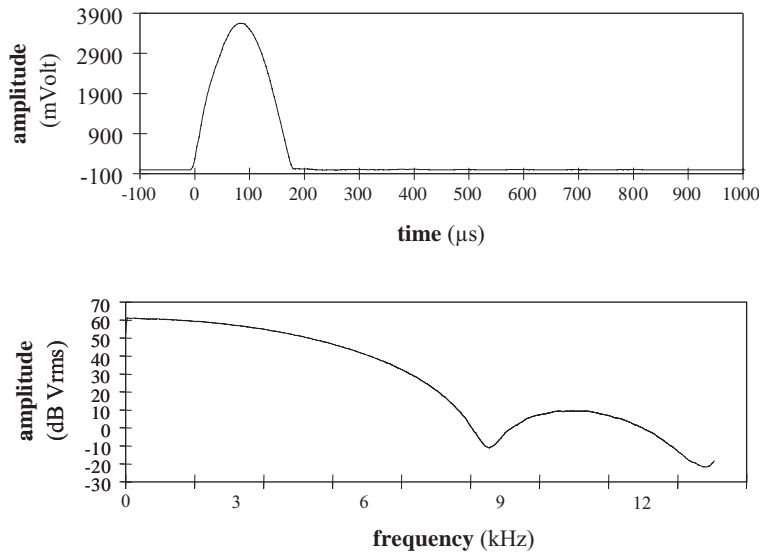


Fig. 3. Time signal (upper) and corresponding frequency spectrum of the impact on a chicken egg.

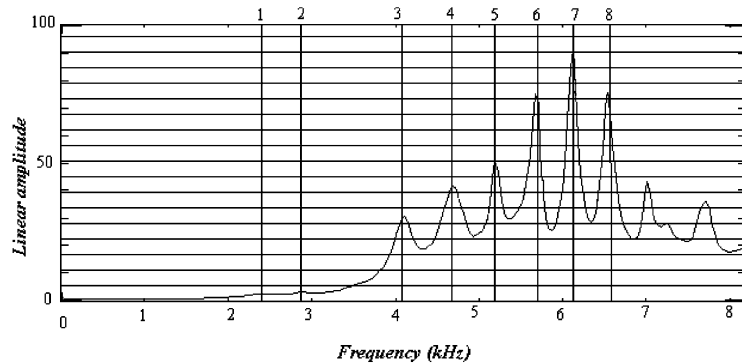


Fig. 4. Global sum of frequency response functions and indication lines of the selected modes.

transformation is a dedicated algorithm to determine the spectral content of a digitized time signal. To achieve high calculation performance, the algorithm requires that the number of time samples ( $N$ ) be a power of two. The measured frequency band ranges from 0 to 12.8 kHz.

The frequency response functions (FRFs) are based on an average of five measurements for each measuring point. In order to assure good-quality measurements, a coherence of more than 90% is required to accept the measurement. These FRFs are used as input data for the experimental modal analysis.

In this test the response is measured at one location on the shell equator while the impacts are made on the 42 measuring points shown in Fig. 1. The set of measured FRFs on a structure can be joined into a frequency response function matrix. This matrix is used as input in the LMS CADA PC software (L.M.S. International n.v., Belgium) that allows the estimation of the modal parameters. Fig. 4 is a global sum of FRFs, which covers the information on all measurements.

### 3. Results

The result of the experimental modal analysis is a set of spherical modes that are characterized by their damped natural frequency, the corresponding damping ratio and the mode shape. This mode shape can be shown in an animated display. The animation consists of rapidly displaying a number of deformed wire frames. The deformation itself varies sinusoidally with an amplitude corresponding to the mode shape vectors of each mode. Figs. 5–7 show momentary shots where the magnitude of the deformation at the antinodal points is maximal. The phase shift between the two pictures of the same mode is 180°. They represent the mode shapes of the most interesting modes. The dark line represents the undeformed egg model. The light grey line is the deformed wire model. Only a relative scaling is used to show the amplitude of the deformation. Table 1 is a list of the dynamic characteristics of the selected modes. The selection of the modes is restricted up to 7 kHz, since the excitation of higher frequencies was not reliable due to the very low-energy content in the higher-frequency range (see Fig. 3). The first column indicates the mode number. The second column is the value for the natural frequency or resonance frequency ( $\omega$ ) of the selected mode. The third column gives the corresponding damping ratio ( $Z$ ).

The first two modes show a shrinking and expanding behaviour of the whole egg. Opposite to the experimental results of Sinha [11] and Yang et al. [2], these modes are not dominant in the total dynamic behaviour of the egg (see Fig. 4).

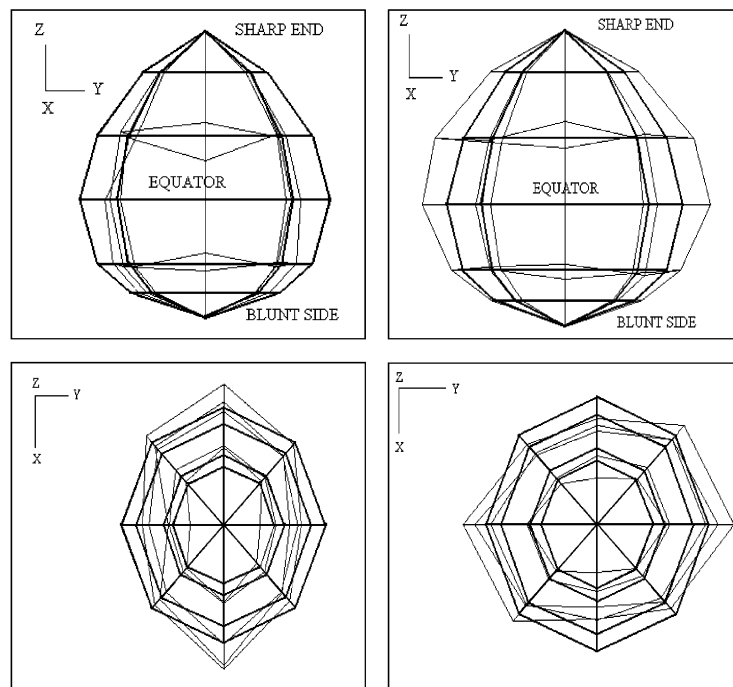


Fig. 5. Front view (top) and top view (below) of the elliptical mode shape (mode no. 3:  $\omega = 4080$  Hz;  $Z = 2.1\%$ ).

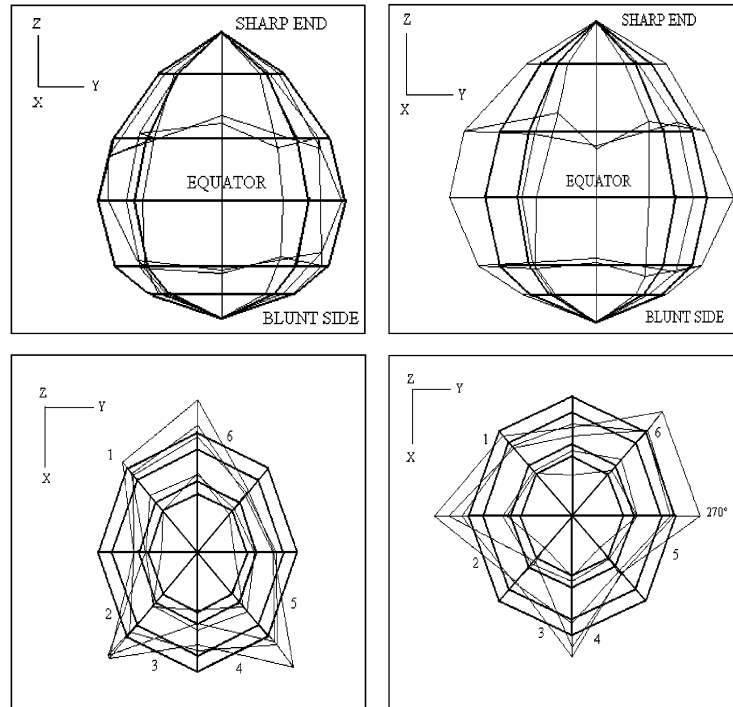


Fig. 6. Front view (top) and top view (below) of the triangular mode shape (mode no. 4;  $\omega = 4667$  Hz;  $Z = 2.34\%$ ).

The first flexural mode has a resonant frequency of 4080 Hz and a corresponding damping ratio of 2.1%. Fig. 5 represents the front and top view of the shape of this mode. This mode is called the oblate–prolate mode. The sharp and blunt sides of the egg do not vibrate. All deformation is concentrated towards the equator zone of the egg. An elliptic shape can be recognized at the equator ring. The amount of deformation decreases gradually towards the poles (blunt and sharp ends) of the egg.

Fig. 6 is a graphical representation of the second observed flexural spherical mode. A triangular deformation shape can be recognized at the equator. Again the poles of the egg have a minimal vibration. The equator zone of the egg shows maximum deformation. The mode shape of this mode is more complex than the previous one. Three nodal lines can be identified, located at the parallels of latitude that intersect the equator ring at locations (1, 4), (2, 5) and (3, 6).

The mode shape of the next mode ( $RF = 5182$  Hz;  $Z = 1.13\%$ ) shows a quadrangular deformation in top view (Fig. 7). Four nodal lines running through the poles of the egg can be identified. These four nodal lines are located at the parallels of latitude that intersect the equator ring at locations (1, 5), (2, 6) and (3, 7) and (4, 8). Fig. 7 is, respectively, a front and top view of the mode shapes.

The mode shapes of the next modes (numbers 6, 7 and 8) are complex and undefined. The excitation of these modes is not reliable, since the energy content of the impact excitation is not high enough. Furthermore, the number of measurement nodes on one parallel of altitude on the eggshell surface is too low to model adequately these mode shapes.



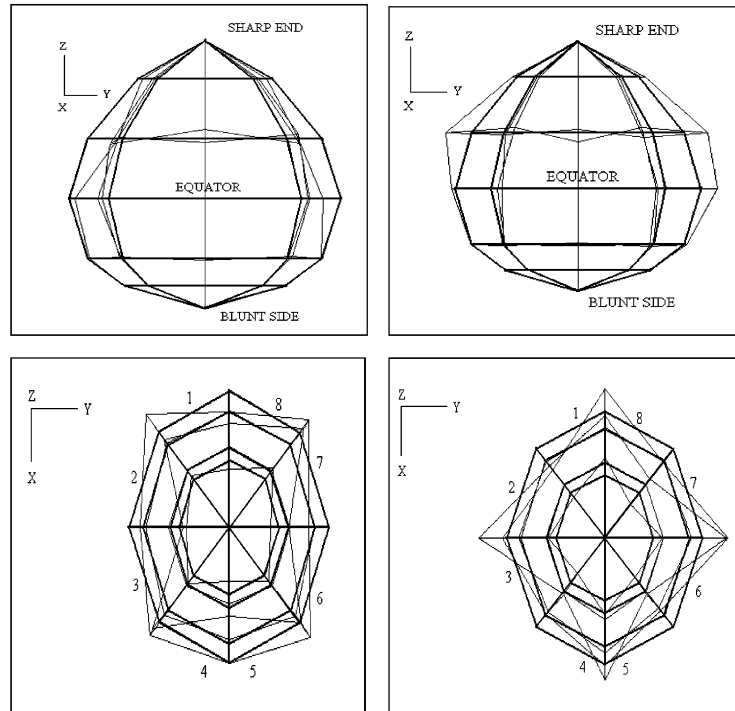


Fig. 7. Front view (top) and top view (below) of the quadrangular mode shape (mode no. 5:  $\omega = 5182$  Hz;  $Z = 1.13\%$ ).

Table 1  
List of selected modes of vibration of an egg

Identification	$\omega$ (Hz)	$Z$ (%)	Description of mode shape
1	2399	11.5	Shrinking and expanding behaviour
2	2862	2.69	Shrinking and expanding behaviour
3	4080	2.10	Elliptic deformation
4	4667	2.34	Triangular deformation
5	5182	1.13	Quadrangular deformation
6	5689	0.85	Complex, undefined mode shape
7	6114	0.79	Complex, undefined mode shape
8	6534	0.77	Complex, undefined mode shape

#### 4. Conclusions

The most interesting frequency range is situated between 4–7 kHz. This confirms the finite element simulations of the whole egg done by Sinha [11]. A whole set of flexural spherical modes was observed.

The flexural spherical mode shapes are very similar to those observed for spherically shaped objects [6], for the inextensional modes of cylindrical objects [12] and in ring structures [13]. The

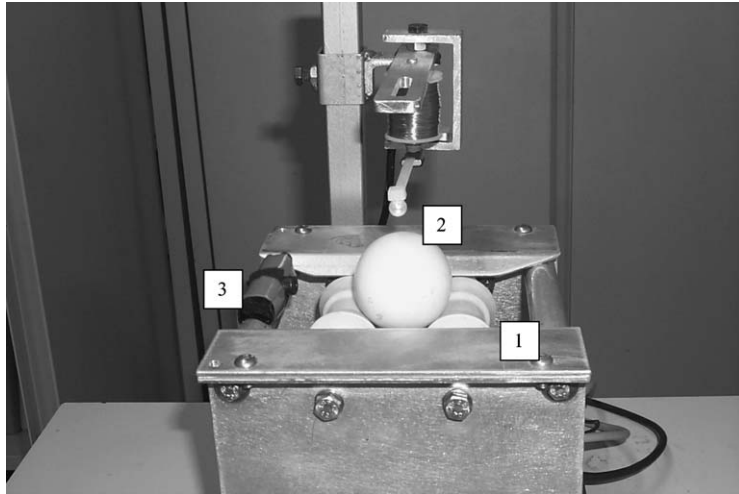


Fig. 8. The lab-scale test arrangement for eggshell breakage inspection, with egg support by diablo-shaped rollers (1), the impacting rod (2) and the microphone (3), located at  $90^\circ$  from the impactor.

complexity of the mode shapes increases with higher frequencies. The analysis of mode shapes of all modes observed in this frequency range indicates that the deformation of the eggshell during vibration is mainly concentrated near the equator zone of the egg. The amplitude of the deformation of each observed mode is maximal at certain points on the equator (antinodal points) and decreases towards the poles of the egg (the sharp and blunt side). This can be explained by the difference in mechanical stiffness between the poles and the equator. Due to the difference in curvature and shell thickness, the poles of the egg are much stiffer than the equator zone and hence the deformation at the poles is smaller.

The study described above opens the door towards the use of egg vibration analysis for non-destructive eggshell crack detection. Since an intact egg is symmetric around its long axis, tapping on different locations on the equator leads to a very repetitive response. The presence of a crack disturbs this symmetry, giving rise to a different response when tapping on different places. A lab-scale prototype is under construction and different classification algorithms will be evaluated. Fig. 8 gives a schematic view of this prototype. The egg is laid down horizontally and supported at the observed nodal lines of the elliptical mode. This is achieved by using diablo-shaped rollers. The point of contact of these rollers with the eggshell coincides with the parallels of latitude of the nodal lines of the elliptical mode. The selection of this support configuration has consequences on the artificial suppression of vibration of the triangular mode as the nodal points of this mode do not coincide with those of the elliptical mode. Instead of using a laser vibrometer as response sensor a contactless low-cost microphone can be used.

### Acknowledgements

The first author wants to thank the Flemish Institute for Scientific and Technological Research and the Belgium Ministry of Agriculture for their financial support. Part of the fundings came in

from the IWT (Instituut voor de Bevordering van het Wetenschappelijk Technologisch Onderzoek in Vlaanderen) through Doctoral Grant No. 942019 and from the FWO (Fonds voor Wetenschappelijk Onderzoek–Vlaanderen) through Grant No. G.0221.00.

## References

- [1] D.N. Sinha, R.G. Johnston, W.K. Grace, C.L. Lemanski, Acoustic resonances in chicken eggs, *Biotechnology Progress* (1992) 240–243.
- [2] S.H. Yang, C. Hsi-Lung, W. Chunghwa, Quality control on thousand year egg by vibration identification, in: *Proceedings of the 13th International Modal Analysis Conference*, Nashville, TN, 1995, pp. 1242–1247.
- [3] G.N. Bliss, Crack detector, U.S. Patent 3744299, 1973.
- [4] A. Moayeri, Probe, device and method for testing eggs, U.S. Patent 5728939, 1997.
- [5] G. Van Woensel, E. Verdonck, R. Snoeys, J. De Baerdemaeker, Measuring the mechanical properties of apple tissue using modal analysis, *Journal of Food Process Engineering* 10 (1984) 151–163.
- [6] L. Huarng, P. Chen, S. Upadhyaya, Determination of acoustic vibration modes in apples, *Transactions of the ASAE* 36 (5) (1992) 1423–1429.
- [7] H. Chen, J. De Baerdemaeker, Modal analysis of the dynamic behavior of pineapples and its relation to fruit firmness, *Transactions of the ASAE* 36 (5) (1994) 1439–1444.
- [8] J. Langenakens, H. Ramon, J. De Baerdemaeker, A model for measuring the effect of tire pressure and driving speed on horizontal sprayer boom movements and spray pattern, *Transactions of the ASAE* 38 (1) (1995) 65–72.
- [9] W. Heylen, S. Lammens, P. Sas, *Modal Analysis Theory and Practice, Course on Modal Analysis Theory and Practice*, Leuven, Belgium, 1993, pp. 1–167.
- [10] M.E. Patton, M.W. Trethewey, A survey and assessment of nonintrusive modal testing techniques for ultra lightweight structures, *Journal of Modal Analysis* 2 (4) (1987) 163–173.
- [11] D.N. Sinha, Personal communication by telephone, 1994.
- [12] Y.G. Tsuei, C.L. Shen, J. Liu, Inextensional modes of circular cylinder, in: *Proceedings of the Fifth International Modal Analysis Conference*, Vol. II, London, 1987, pp. 896–902.
- [13] R.D. Blevins, *Formulas for Natural Frequency and Mode Shapes*, Krieger Publishing Company, Florida, USA, 1993, pp. 204.